

Electronic Supplementary Information. Ectoine Interaction with DNA: Influence on Ultraviolet Radiation Damage

Marc Benjamin Hahn^{*1,2}, Glen J. Smales², Harald Seitz^{3,4},
Tihomir Solomun², and Heinz Sturm²

¹Freie Universität Berlin, Institut für Experimentalphysik, 14195
Berlin, Germany

²Bundesanstalt für Materialforschung und -prüfung, 12205 Berlin,
Germany

³Universität Potsdam, Institut für Biochemie und Biologie, 14476
Potsdam, Germany

⁴Fraunhofer Institute for Cell Therapy and Immunology, 14476
Potsdam, Germany

DNA damage data extracted from agarose gel electrophoresis

Table 1: Overview of the irradiation results. Given are laser wavelength (λ), the fluence (F), the cosolute present, the buffer solution, the percentage of supercoiled plasmids present in the respective gel lanes, without digest (SSB), and after enzyme treatment (T4) and the sample size (n). All errors represent the standard deviation calculated from n samples.

λ/nm	F/Jcm^{-2}	Cosolute	Solvent	$SC_{SSB}/\%$	$SC_{T4}/\%$	n
-	0	-	PBS	89±04	70±05	6
266	20	-	PBS	82±05	14±04	4
266	20	Ectoine	PBS	85±06	37±06	4
266	20	Hyd.Ect.	PBS	82±05	35±14	4
-	0	-	Water	81±03	63±04	6
266	20	-	Water	50±06	31±11	4
266	20	Ectoine	Water	63±06	28±17	4
266	20	Hyd.Ect.	Water	62±05	28±14	4

*hahn@physik.fu-berlin.de

The method to calculate the attachment efficiencies of DNA dyes to plasmid DNA of different conformation

The difference in the attachment efficiency of DNA dyes to the supercoiled plasmids in comparison to the open circular and linear plasmids can be determined as follows. The method is similar to the method described in the literature.¹ Here we make the following assumptions:

The total amount N of plasmids in all lanes (a-x) are the same:

$$N^a = N^b = \dots = N^x \quad (1)$$

N is the sum over all plasmids in supercoiled conformation N_1 and opencircular or linear conformation N_2 :

$$N = N_1 + N_2 \quad (2)$$

Here we assume that the dye has the same attachment efficiency to the plasmids in the opencircular and linear conformation. The total measured fluorescence intensity of all bands I is the sum of the intensities originating from either plasmids in supercoiled I_1 or opencircular and linear conformation I_2 :

$$I = I_1 + I_2 \quad (3)$$

We assume that the relation between the fluorescence intensity is linear in the amount of attached dyes to the plasmids and that the attachment is homogeneous that we can write:

$$I_1 = c_1 N_1 \quad (4)$$

and

$$I_2 = c_2 N_2 \quad (5)$$

with c_1 and c_2 as the respective attachment efficiencies. By combination of the eq. 1 to eq. 5 it follows that

$$I_1^a + \frac{c_1}{c_2} I_2^a = I_1^b + \frac{c_1}{c_2} I_2^b. \quad (6)$$

Here a, b and x stand for the respective lane in the gel. The intensities I_n^x can be directly extracted from the gel image.

$$\frac{c_1}{c_2} = \frac{I_1^a - I_1^b}{I_2^b - I_2^a}. \quad (7)$$

Therefore the value of interest, the ratio between the attachment efficiencies c_1/c_2 of the dye can be determined from gel images with plasmids in its native form and linearized form by an enzyme digest as shown in fig. 1.

The results for SYBR gold attachment efficiency to pUC19

The intensity profiles of the different lanes were extracted from the gel image, a linear background subtracted, and voigt multipeak fitting was performed using the Fityk software.² The ratio of c_1/c_2 was calculated according to eq. 7 for each two neighbouring lanes. The results (n=8) were averaged and the standard error calculated as 0.11. We can conclude that within the accuracy of the measured values, the ratio of the attachment efficiency of *SYBR gold* to the different conformations of plasmid DNA *pUC19* is

$$\frac{c_1}{c_2} = 1.05 \pm 0.11. \quad (8)$$

Therefore no correction is needed for the different fluorescence intensities.

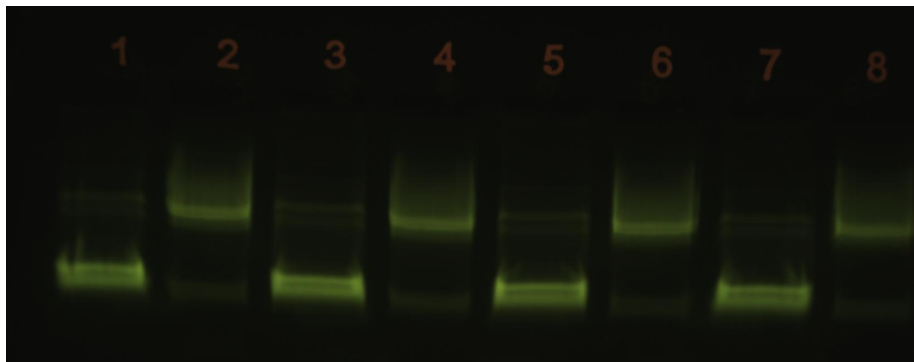


Figure 1: Agarose gel image with native plasmid (*pUC19*) in lanes with odd number and *HindIII* digested plasmid in lanes with even numbers. For details on the gel, see main text.

Change of DNA melting temperature by ectoine and hydroxyectoine

The results of the melting temperature measurements in PBS are for pure DNA $T_m = 84.2 \pm 0.4$ ($R^2 = 0.981$), for ectoine $T_m = 82.7 \pm 0.4$ ($R^2 = 0.996$) and for hydroxyectoine $T_m = 81.6 \pm 0.7$ ($R^2 = 0.988$). From the literature it is known, that ectoine lowers the melting temperature of DNA.³⁻⁵ For hydroxyectoine, a lowering⁵, no change³ as well as an increase⁴ of DNA melting temperature was reported. To clarify the situation regarding hydroxyectoine and analyse our data in a coherent manner, we measured the influence of ectoine and hydroxyectoine on DNA melting temperature in PBS. Supercoiled plasmid DNA is suspect to torsional stress which influences melting behaviour. Therefore, pUC19 dsDNA was linearised (*HindIII*, Jena Bioscience) and complete linearisation was checked with agarose gel electrophoresis. Measurements were performed in an UV-vis spectrometer (UV-2101, Hamamatsu) and suprasil cuvettes (Hellma Analytics). Heating was performed with a cuvette heating cell with a digital temperature controller attached (Pike technologies). After equilibration, UV spectra were acquired between 310 nm-240 nm. Temperature was measured with a Pt thermocouple within the cuvette. To account for the cosolute signal at 260 nm, the relative absorbance was calculated as: $Abs = Abs_{260\text{ nm}} - Abs_{290\text{ nm}}$. Plasmid DNA concentration was 20 ng/ μL in PBS. The ectoine and hydroxyectoine concentrations were 125 mmol/L. The melting temperature (T_m) of the linearised plasmid DNA in PBS were determined from the melting curves and a sigmoidal curve fit to the relative absorbance ($Abs(T) = Abs_0 + C/(1 + e^{((T-T_m)/\kappa)})$) with the temperature (T), and fitting parameters (C, κ).

Electron paramagnetic resonance measurements

To determine the radical scavenging capabilities of the cosolutes, EPR measurements were performed. For the EPR measurements, a X-band Miniscope MS300 spectrometer (Magnettech) in combination with disposable capillaries (Ringcaps 50 μL sealed with Critoseal, Hirschmann) was used. The field centre was set to 3358 G, field sweep to 98 G, sweep time to 15 s, modulation to 2000 mG, MW attenuation to 5 dB, gain to 5×10^2 dB, and automatic frequency

control was activated. Ten spectra were averaged for each measurement. Glycine betaine, H_2O_2 , FeSO_4 , and, 5,5-dimethyl-1-pyrroline-n-oxide (DMPO for EPR spectroscopy) were purchased from Sigma Aldrich. Hydroxyl radicals were produced by Fenton's reaction similar to the experiments concerning the radical scavenging properties of ectoine as described in detail in our previous work.⁶ immediately before the EPR measurements, 35 μL of ultra pure water or 3 mol/L ectoine, hydroxyectoine, tris or glycine betaine solution were mixed with 2 μL DMPO (1M) and 2 μL FeSO_4 (1mM). To initiate Fenton's reaction, 2 μL of 10mM H_2O_2 was added and the solutions were immediately transferred to the capillaries. The time between mixing of the reagents and accumulation of the first spectra was 40 ± 20 s. Due to the absence of the EPR signal by tris under the above conditions, additional measurements were performed with adjusted solute ratios: 35 μL DMPO, 2 μL tris, 2 μL H_2O_2 and 2 μL FeSO_4 .

Radical scavenging by ectoine, hydroxyectoine and tris

The EPR measurements of the $\bullet\text{OH}$ -radicals, produced by Fenton's reaction, showed for pure water the four characteristic OH-DMPO peaks (fig 2). In the

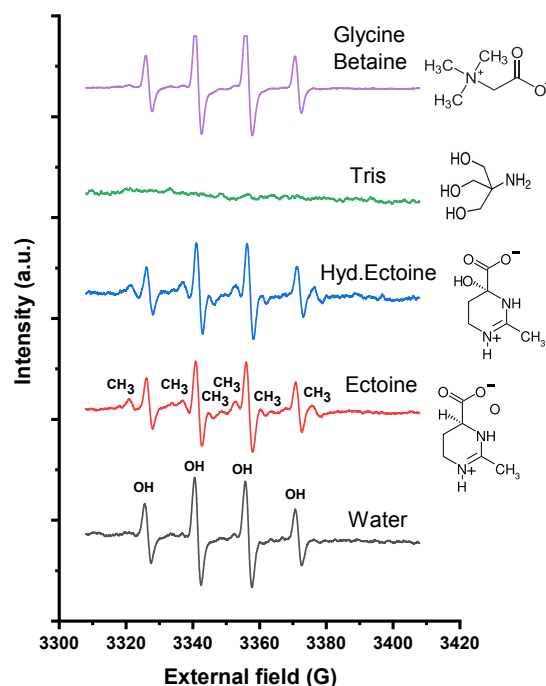


Figure 2: EPR spectra of OH-DMPO and CH_3 -DMPO radicals produced by Fenton's reaction and various cosolutes together with their respective chemical structures. The positions of the four OH-DMPO (OH) and six CH_3 -DMPO (CH_3) peaks are marked in the spectra of pure water and ectoine only for reasons of clarity. With the exception of tris, all spectra are normalised on the maximum of the first OH-DMPO peak. From top to bottom: Glycine betaine, tris, hydroxyectoine, ectoine and pure water spectra with the same molar and DMPO concentrations.

presence of ectoine additionally six CH_3 -DMPO peaks appeared as already dis-

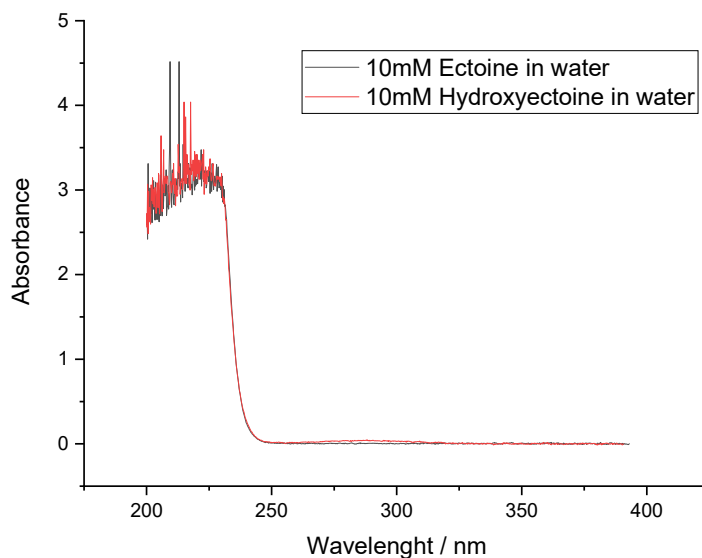


Figure 3: Shown is the absorbance of ectoine and hydroxyectoine at 10mM concentration in water.

cussed in detail in our previous work.⁶ For hydroxyectoine, similarly six CH_3 -DMPO peaks were detected as expected due to the similarities in molecular structure between the two ectoines as displayed in fig 2, next to the respective spectra. These peaks are the result of the OH-scavenging of ectoine and hydroxyectoine by CH_3 abstraction and the subsequent formation of the CH_3 -DMPO compounds.^{6,7} For glycine betaine, which is known not to be an effective radical scavenger, no additional signal from scavenging reactions was detected.⁶ In contrast, measurements with the well known and effective scavenger tris for the same EPR settings and reagent concentrations, no EPR signal could be detected (shown in fig. 2 as "tris"). A decrease in tris concentration and an increase in DMPO concentration lead to the observation of a rather low EPR signal with a variety of peaks (data not shown). We attribute this behaviour to a shift in the competitive scavenging reactions of tris and DMPO in favour of DMPO compared to the measurement with higher tris and lower DMPO concentrations. This indicates the well known and effective scavenging of $\bullet\text{OH}$ -radicals by tris,⁷ as well as the absence of formation of secondary scavenging products, which form long lived radicals with DMPO.

Ectoine UV absorption

All UV absorption measurements were performed in a dual beam UV-vis spectrometer (UV-2101, Hamamatsu) in UV cuvettes with 10 mm path length (100-QS Suprasil, Hellma), a slit width of 1 nm, sampling interval of 0.2 nm, baseline correction and a deuterium lamp. After a linear background subtraction the absorbance was determined at 355 nm 300 nm and 266 nm for all presented ectoine and hydroxyectoine concentrations. A least square fit to the

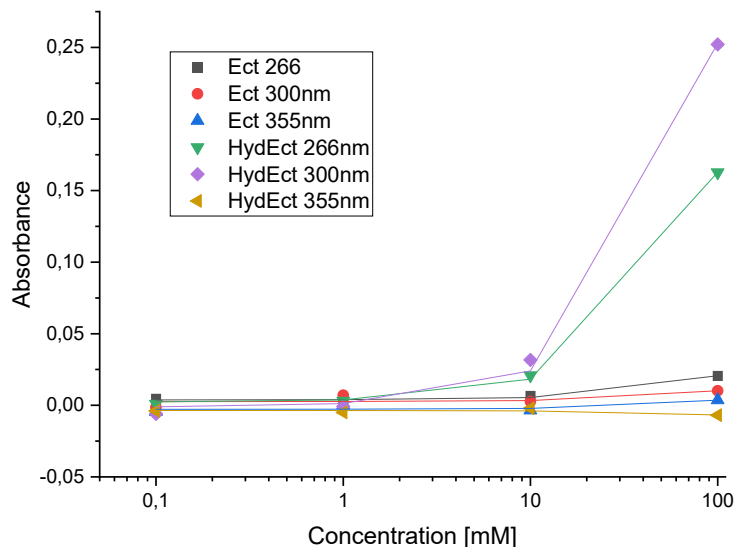


Figure 4: Shown is the concentration dependent UV absorbance of Ectoine and Hydroxyectoine at three different wavelength 266 nm (UV-C), 300 nm (UV-B) and 355 nm (UV-A). The lines are guide to the eyes.

absorption data as presented in fig. 4 resulted in the molar attenuation coefficients as given in tab. 2. From this data we can conclude that the absorption of ectoine (at 10mM concentration as used during the irradiation experiments ($Abs_{Ect} = (1.6 \pm 2) \cdot 10^{-3}$) is neglectable when compared to the DNA at concentrations of $17 \mu\text{g/mL}$ and $Abs_{dsDNA} \approx 0.3$ (with the assumption of the standard value of $Abs_{dsDNA} = 1$ for dsDNA at concentrations of $50 \mu\text{g/mL}$).

References

- [1] Michael F Shubsda, Jerry Goodisman, and James C Dabrowiak. Quantitation of ethidium-stained closed circular DNA in agarose gels. *Journal of Biochemical and Biophysical Methods*, 34(1):73–79, February 1997.
- [2] Marcin Wojdyr. Fityk : A general-purpose peak fitting program. *Journal of Applied Crystallography*, 43(5):1126–1128, October 2010.
- [3] Gennady Malin, Robert Iakobashvili, and Aviva Lapidot. Effect of Tetrahydropyrimidine Derivatives on Protein-Nucleic Acids Interaction Type II Restriction Endonucleases as a Model System. *Journal of Biological Chemistry*, 274(11):6920–6929, December 1999.
- [4] Michael Schnoor, Peter Voß, Paul Cullen, Thomas Böking, Hans-Joachim Galla, Erwin A. Galinski, and Stefan Lorkowski. Characterization of the synthetic compatible solute homoectoine as a potent PCR enhancer. *Biochemical and Biophysical Research Communications*, 322(3):867–872, September 2004.

Type	Wavelength [nm]	Molar attenuation coefficient	R ²
Unit	nm	mmol ⁻¹ cm10 ⁻¹	-
Ectoine	266	$(1.6 \pm 0.2)10^{-4}$	0.97
Ectoine	300	$(8 \pm 5)10^{-5}$	0.53
Ectoine	355	$(6 \pm 3)10^{-5}$	0.68
Hydroxyectoine	266	$(1.61 \pm 0.03)10^{-3}$	0.99
Hydroxyectoine	300	$(2.54 \pm 0.008)10^{-3}$	0.99
Hydroxyectoine	355	$(-3 \pm 2)10^{-5}$	0.56

Table 2: Molar attenuation (together with the standard error) for ectoine and hydroxyectoine at different wavelength. We note here, that the values at 355 nm result from datapoints which were within the noise range and are therefore only included for completeness.

- [5] Matthias Kurz. Compatible solute influence on nucleic acids: Many questions but few answers. *Saline Systems*, 4:6, June 2008.
- [6] Marc Benjamin Hahn, Susann Meyer, Maria-Astrid Schröter, Hans-Jörg Kunte, Tihomir Solomun, and Heinz Sturm. DNA protection by ectoine from ionizing radiation: Molecular mechanisms. *Physical Chemistry Chemical Physics*, 19(37):25717–25722, September 2017.
- [7] Clemens von Sonntag. *Free-Radical-Induced DNA Damage and Its Repair*. Springer, Berlin, Heidelberg, 2006.